A Comparison of Enthalpy Values of Selected Metals Obtained by Pulse-Heating and Differential-Scanning-Calorimetry [1]

B. Wilthan [2], C. Cagran [2] and G. Pottlacher [2,3]

[1] Paper presented at the 15th Symposium on Thermophysical Properties, Boulder, Colorado, U.S.A., June 22-27, 2003.

[2] Institut für Experimentalphysik, Technische Universität Graz, Petersgasse 16, A – 8010 Graz, Austria.

[3] To whom correspondence should be addressed.

ABSTRACT
Measurements of thermophysical properties enthalpy, electrical resistivity and specific heat capacity as a function of temperature starting from the solid state up into the liquid phase for Fe, Ni and Pt are presented within this work. Two different measurement approaches have been used within this work: An ohmic pulse heating technique, which allows - among others - the measurement of enthalpy, specific heat capacity and electrical resistivity up to the end of the stable liquid phase, and a differential – scanning – calorimetry technique (DSC) which enables determination of specific heat capacity from almost room temperature up to 1500 K. The microsecond ohmic pulse heating technique uses heating rates up to 10^8 K/s and thus is a dynamic measurement, whereas the differential – scanning – calorimetry technique uses heating rates of typically 20 K/min and can be considered as a quasi-static process. Despite the different heating rates both methods give a good agreement of the thermophysical data within the stated uncertainties of each experiment.
Within this work results on the metals Fe, Ni and Pt are reported. The investigated enthalpy and resistivity data as a function of temperature are presented and compared to literature-values.

KEY WORDS: DSC, electrical resistivity, enthalpy, iron, nickel, platinum, pulse-heating, specific heat.

1 INTRODUCTION

Thermophysical data such as enthalpy and electrical resistivity as a function of temperature of metals and alloys have been measured for many years at the Institut für Experimentalphysik in Graz by using various fast pulse heating techniques at different time scales (heating rates applied 10^8 - 10^9 $K \cdot s^{-1}$) [1]. Within our pulse-heating experiments on wire samples temperature is determined by means of fast optical pyrometers, they have a response time of about 100 ns. The monochromatic instruments may use two different detectors, namely a Si diode or an InGaAs diode. Since monochromatic pyrometers usually are "self-calibrated" with the plateau of the melting transition of the investigated metal, high sensitivity is desirable. A wide temperature range in a single measurement is possible with the use of a fast operational amplifier with a linear output. But when using such a fast optical pyrometer under pulse heating conditions, there are some mayor restrictions to the onset temperature of such a fast device. For a short rise time the active area of the device has to be very small e. g. 1 x 1 mm, also the interference will limit the amount of light that reaches the detector. Because of shielding reasons the pyrometer has to be housed in a shielded box, and the light of the radiating sample is conducted to it via optical light-guides, finally there are losses due to reflection at the windows of the experimental chamber and at the lenses of the pyrometer, which all together strongly will decrease the flux of light that finally reaches the detector and result in a lowest detectable temperature of our pyrometers of about 1200 to 1500 K. Therefore all thermophysical properties published earlier e.g. [1], [2] started at temperatures between 1200 K and 1500 K.

Other than the pyrometric determined temperature, all other basic measurements are electrical signals (current trough the sample, voltage drop across the specimen) an thus not limited to certain temperature ranges. Therefore we are able to measure these electrical signals over the entire range covered by the pulse-heating experiment starting from room temperature up to the end of the stable liquid phase.

As a result, evaluated thermophysical properties like enthalpy and electrical resistivity can generally be calculated over the entire temperature range, but the onset temperature of the pyrometers (of about 1200 K – 1500 K) limits the possibility to depict these quantities versus temperature to the range above the pyrometer onset, which is in fact a strong limitation.

To overcome this limitation and to obtain temperature dependencies for these quantities below the onset-temperature of the pyrometers a differential scanning calorimeter (DSC) NETZSCH DSC 404 was added to our setup and incorporated into the basic measurement routines for data in the temperature range of about 500 K – 1500 K. The DSC is able to perform accurate specific heat capacity measurements in the above mentioned temperature range. The results are combined with those of the pulse heating experiments by using the enthalpy versus temperature dependency of the DSC to expand the temperature range of the pulse-heating data. Thus, temperature dependencies of all thermophysical properties can be down scaled to the DSC-onset temperature of about 500 K.

2 MEASUREMENTS

2.1 Pulse Heating with Microsecond Time Resolution

The optics of the pyrometer views an area of 0.2 mm x 10 mm of the pulse heated sample surface (sample dimensions 50 mm length, 0.5 mm diameter) with a 1:1 magnification onto the rectangular entry slit of an optical waveguide. The interference filter with a center wavelength of 650 nm and a half power bandwidth of 37 nm is in front of the entry slit of the waveguide. The light delivered by this waveguide is detected by a Si - photodiode and amplified with a fast amplifier (bandwidth 1 MHz). The intensity signal J can be expressed as:

$$J(l,T) = g \cdot s(l) \cdot t(l) \cdot e_l(l,T) \cdot \frac{c_1}{l^5 \left[e^{\frac{c_2}{l \cdot T}} - 1 \right]} \tag{1}$$

where the symbols are given as g, geometry factor; s, sensitivity of electronics and diode; l, wavelength; t, transmission of optic and optical waveguide; $e_?$, normal spectral emissivity, c_1 and c_2, first and second radiation constant; T, temperature.
By forming ratios of the measured radiance intensity at melting $J(T_M)$ and the measured radiance intensity $J(T)$ at temperature T, one obtains the unknown temperature T with the melting temperature of the investigated material as the calibration point:

$$T = \frac{c_2}{l \ln\left\{1 + \frac{J_m(T_M)\, e(l,T)}{J(T)\, e(l,T_M)} \left[\exp\left(\frac{c_2}{l T_M} \right) - 1 \right]\right\}} \tag{2}$$

where $e(l,T)$ is the emissivity of the liquid sample and $e(l,T_M)$ is the emissivity at the melting temperature. For emissivity dependencies of liquid metals see e.g. [3], [4].

The temperature range covered by the optical pyrometer is from about 1200 K up to about 5000 K, depending on the material under investigation. Thus the experiments lead far into the metal's liquid phase. The stability limit of the pulse heated wire sample for this type of experiment is the boiling of the sample. During one fast pulse experiment by measuring the current through the sample, the voltage drop across it and the radiation temperature of it, one may obtain data for the enthalpy, temperature and electric resistivity as the specimen rapidly passes through a wide range of states from room temperature up into the liquid phase. From these quantities the specific heat at constant pressure, thermal conductivity and thermal diffusivity may be calculated. For more details on the experiment and on data reduction see e.g. [1].

2.2 DSC – Measurements

The DSC allows primarily to measure the heat capacity of the sample (5.2 mm diameter and 0.5 mm height) in a given temperature range. The sample is measured relatively to a

second, inert sample of approximately the same heat capacity. One experiment consists usually of three separate runs: a scan with two empty pans, a scan with one pan containing a reference sample from sapphire and finally a scan with the sample in the same pan where the reference sample was before. The heat capacity as a function of temperature of the sample under investigation, $c_p(T)$, is obtained by using the following equation:

$$c_p(T) = c_p^{\mathrm{r}}(T)\frac{m^{\mathrm{r}}}{m}\frac{\Delta_3 - \Delta_1}{\Delta_2 - \Delta_1} \tag{3}$$

where Δ1, Δ2, Δ3 are the three DSC signals with empty pans, the signal of the reference and the signal of the sample itself. m^r, and m are the masses of the reference and the sample respectively, and c^r_p is the heat capacity of the reference.
Using this heat capacity $c_p(T)$ obtained with DSC measurements one is able to calculate the enthalpy of the specimen by integrating the heat capacity signal and adding the room temperature enthalpy $H_{(298)}$ to the result:

$$H_{298}(T) = \int_{473}^{T} c_p(T)\cdot dT + (473-298)\cdot c_p(473) \tag{4}$$

$H(T)$ is the enthalpy and c_p the specific heat capacity.
Therefore, the enthalpy versus temperature dependency for a given material can be calculated directly from the DSC measurements. This enthalpy to temperature dependency can further be used to obtain the inverse dependency, temperature versus enthalpy. With this result, we are able to down scale our electrical measurements (i.e. enthalpy or electrical resistivity) of the pulse heating experiment by combining the temperature scale from the DSC (Temperature vs. Enthalpy) with the electrical measured properties versus enthalpy. It has to be stated, that the above mentioned procedure is only useable, as long as there are no phase transitions in the solid sate of the material under investigation. Phase transitions can easily be observed within DSC measurements, but are mostly invisible under pulse-heating conditions as applied within this experiment, due to the extreme high heating rates of 10^8 K·s^{-1}. This procedure enables us to extend the graphs enthalpy versus temperature and resistivity versus temperature to lower temperature regions, starting now at the onset temperature of the DSC (500 K). Up to now the access to these temperature regions when using pulse heating techniques was only possible by experiments with millisecond time resolution [5].

3 RESULTS

In agreement with literature values we used the following melting temperatures for data evaluation: Nickel: 1728 K [6], Iron: 1808 K [7], Platin: 2042 K [8] and Tungsten: 3693K.

Platinum

In Figure 1 specific enthalpy versus temperature for platinum is shown. In the temperature range from 473 K < T < 1573 K we obtain from our DSC-measurements the following fit:

$$H(T) = -38.689 + 0.127 \cdot T + 1.344 \cdot 10^{-5} \cdot T^2, \quad (5)$$

where H is in $kJ \cdot kg^{-1}$ and T in K, also for all following H versus T fits ((6), (7), (14), (15), (16), (21), (22)).
The linear fit for solid platinum in the temperature range 1700 K < T < 2040 K is obtained from 11 independent pulse-heating measurements:

$$H(T) = - 96.075 + 0.180 \cdot T, \quad (6)$$

For the liquid in the temperature range 2045 K < T < 2830 K we obtain again from 11 pulse heating measurements

$$H(T) = 1.636 + 0.187 \cdot T. \quad (7)$$

Figure 2 presents specific electrical resistivity with initial geometry, $r_{el,\,IG}$, not compensated for thermal expansion as a function of temperature for platinum. In the temperature range from 473 K < T < 1573 K we obtain from our DSC-measurement the following fit

$$r_{el,\,IG}(T) = -0.018 + 4.464 \cdot 10^{-4} \cdot T - 6.955 \cdot 10^{-8} \cdot T^2, \quad (8)$$

where $r_{el,\,IG}$ is in $\mu\Omega \cdot m$ and T in K, also for all following $r(T)$ (9, 10, 11, 12, 13, etc).
The linear fit to our values for the solid in the temperature range 1740 K < T < 2042 K is

$$r_{el,\,IG}(T) = 0.155 + 2.229 \cdot 10^{-4} \cdot T, \quad (9)$$

for the liquid in the temperature range 2042 K < T < 2900 K

$$r_{el,\,IG}(T) = 0.854 + 2.713 \cdot 10^{-5} \cdot T. \quad (10)$$

In Figure 2 specific electrical resistivity with volume expansion considered, $r_{el,\,VOL}$ is additionally plotted as a function of temperature. The polynomial fit to our specific electrical resistivity with volume expansion considered, $r_{el,\,VOL}$ for the solid in the temperature range 473 K < T < 1600 K is:

$$r_{el,\,VOL}(T) = -0.01633 + 4.39347 \cdot 10^{-4} \cdot T - 5.69652 \cdot 10^{-8} \cdot T^2, \quad (11)$$

for 1740 K < T < 2042 K

$$r_{el,\,VOL}(T) = 0.161 + 2.132 \cdot 10^{-4} \cdot T + 1.219 \cdot 10^{-8} \cdot T^2, \quad (12)$$

and for the liquid in the temperature range 2042 K < T < 2900 K

$$r_{el,\,VOL}(T) = 0.842 + 5.926 \cdot 10^{-5} \cdot T + 1.154 \cdot 10^{-8} \cdot T. \quad (13)$$

The effect of volume consideration for resistivity is shown as an example for platinum. For all other materials only the resistivity at initial geometry will be presented, as the compensation of volume expansion shifts the resistivity to higher values and can be done with the according volume expansion data available in literature.

Nickel

Figure 3 presents enthalpy versus temperature for nickel. In the temperature range from 473 K < T < 1270 K we obtain from our DSC-measurements the following fit:

$$H(T) = -166.644 + 0.546 \cdot T + 2.394 \cdot 10^{-6} \cdot T^2, \quad (14)$$

the linear fit for solid nickel obtained by pulse-heating in the temperature range 1200 K < T < 1715 K is:

$$H(T) = -272.961 + 0.634 \cdot T, \quad (15)$$

and for the liquid in the temperature range 1740 K < T < 2240 K

$$H(T) = -151.913 + 0.720 \cdot T. \quad (16)$$

Figure 4 depicts electrical resistivity with initial geometry versus temperature for nickel: In the range from 473 K < T < 637 K we obtain from the DSC:

$$r_{el,\,IG}(T) = -0.042 + 2.080 \cdot 10^{-4} \cdot T + 5.126 \cdot 10^{-7} \cdot T^2, \quad (17)$$

and in the range 638 K < T < 1270 K:

$$r_{el,\,IG}(T) = -0.181 + 0.001 \cdot T - 8.197 \cdot 10^{-7} \cdot T^2 + 2.351 \cdot 10^{-10} \cdot T^3. \quad (18)$$

By means of pulse-heating we obtain in the range 1300 K < T < 1715 K

$$r_{el,\,IG}(T) = 0.094 + 3.764 \cdot 10^{-4} \cdot T - 5.644 \cdot 10^{-8} \cdot T^2, \quad (19)$$

and in the range 1750 K < T < 2200 K:

$$r_{el,\,IG}(T) = 0.728 + 2.546 \cdot 10^{-5} \cdot T. \quad (20)$$

Iron

In Figure 5 enthalpy versus temperature for iron is presented. For the temperature range from 473 K < T < 1270 K our DSC-measurements are printed in table 1, as the data can not be described by a polynomial fit.

Table 1: Experimental data for enthalpy versus temperature for solid iron.

T, K	H, kJ·kg^{-1}	T, K	H, kJ·kg^{-1}
473	92.330	1034	478.620
500	106.625	1050	497.253
550	133.844	1066	513.856
600	162.086	1100	543.701
650	191.385	1150	583.496
700	221.806	1187	611.617
750	253.464	1191	615.813
800	286.575	1200	630.727
850	321.450	1205	637.155
900	358.630	1214	644.517
950	398.821	1250	667.282
1000	443.645	1270	679.802

The linear fit for solid iron in the temperature range 1420 K < T < 1790 K obtained by pulse-heating is

$$H(T) = -276.650 + 0.732 \cdot T, \quad (21)$$

for the liquid in the temperature range 1830 K < T < 2370 K we obtain:

$$H(T) = -107.306 + 0.770 \cdot T. \quad (22)$$

Figure 6 depicts electrical resistivity versus temperature for iron, in the range 473 K < T < 1000 K by means of DSC we obtain:

$$r_{el,\,IG}(T) = 0.015 + 1.998 \cdot 10^{-4} \cdot T + 5.433 \cdot 10^{-7} \cdot T^2 + 1.935 \cdot 10^{-10} \cdot T^3, \quad (23)$$

and in the range from 1000 K < T < 1270 K

$$r_{el,\,IG}(T) = -20.603 + 0.053 \cdot T - 4.269 \cdot 10^{-5} \cdot T^2 + 1.161 \cdot 10^{-8} \cdot T^3. \quad (24)$$

By pulse-heating we obtain in the solid range 1250 K < T < 1790 K

$$r_{el,\,IG}(T) = 0.591 + 6.594 \cdot 10^{-4} \cdot T - 1.64763 \cdot 10^{-7} \cdot T^2, \quad (25)$$

and in the liquid range from 1830 K < T < 2370 K

$$r_{el,\,IG}(T) = 1.232 + 2.342 \cdot 10^{-5} \cdot T. \quad (26)$$

4 DISCUSSION

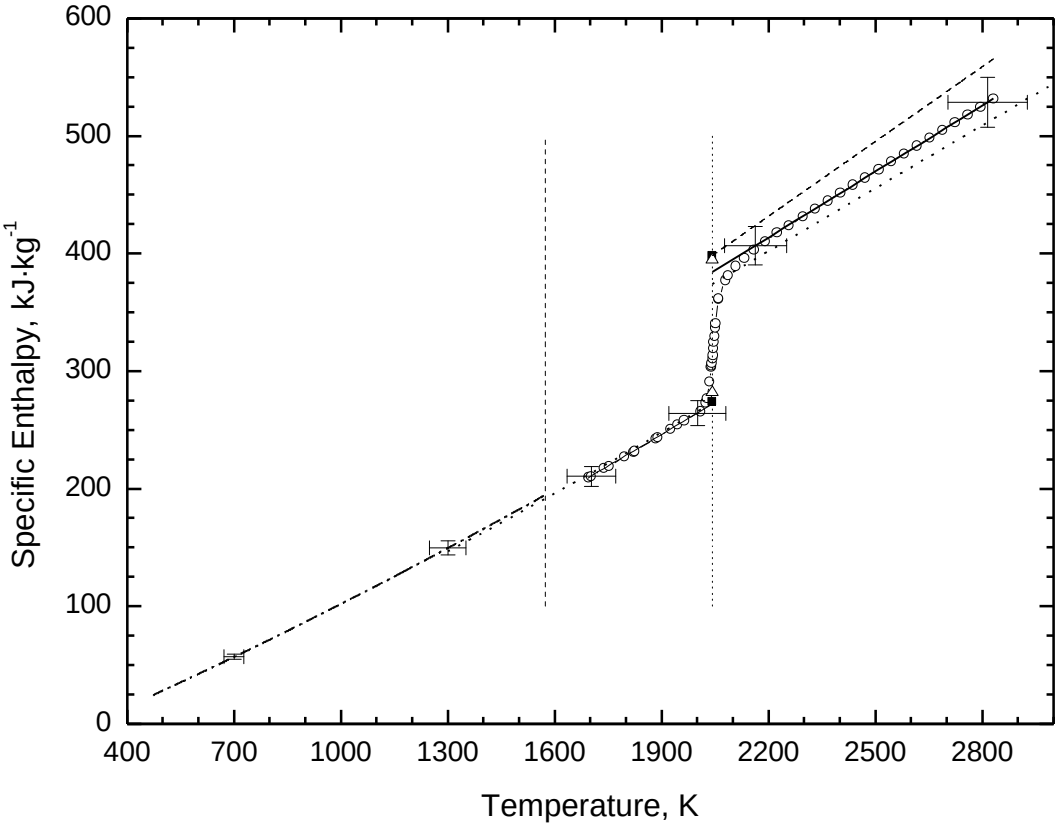

Fig. 1: Specific enthalpy versus temperature for platinum. Open circles represent measured data from this work (average of 11 measurements). Full lines: linear least-squares fits to mean-values of measured data; full squares: values at the begin and the end of melting from Hixson and Winkler [14]; dashed line: literature values for the liquid phase from [14]; vertical dashed line: end of values measured and calculated with DSC-data (1573 K) vertical dotted line: melting temperature (2042 K); open triangle: literature value from Martynyuk [15] at the melting temperature; dotted line: literature values from Hultgren et al. [11]; dashed-dotted line: data from this work (DSC-measurement).

Fig. 1: For the solid platinum we acquire a c_p value of 180 $J \cdot kg^{-1} \cdot K^{-1}$ in the range 1700 K – 2040 K. Seville [9] reports a value of 187.5 $J \cdot kg^{-1} \cdot K^{-1}$ at 1850 K, Righini and Rosso [10] report a value of 189 $J \cdot kg^{-1} \cdot K^{-1}$ at 2000 K, and at the onset of melting Hultgren et. al. [11] report 179.6 $J \cdot kg^{-1} \cdot K^{-1}$. For the liquid we acquire a c_p value of 187 $J \cdot kg^{-1} \cdot K^{-1}$, Margrave [12] reports a value of 186.7 $J \cdot kg^{-1} \cdot K^{-1}$, Chaudhuri et al. [13] report a value of 186 $J \cdot kg^{-1} \cdot K^{-1}$ obtained by levitation calorimetry. Hixson and Winkler [14] report 211.9 $J \cdot kg^{-1} \cdot K^{-1}$ at a pressure of 2000 bar obtained by pulse heating and the data-collection of Hultgren et. al. [11] recommends 178.1 $J \cdot kg^{-1} \cdot K^{-1}$.
The measured values give a very good agreement to the literature values as well in the solid phase as for the liquid phase within the uncertainty bars.

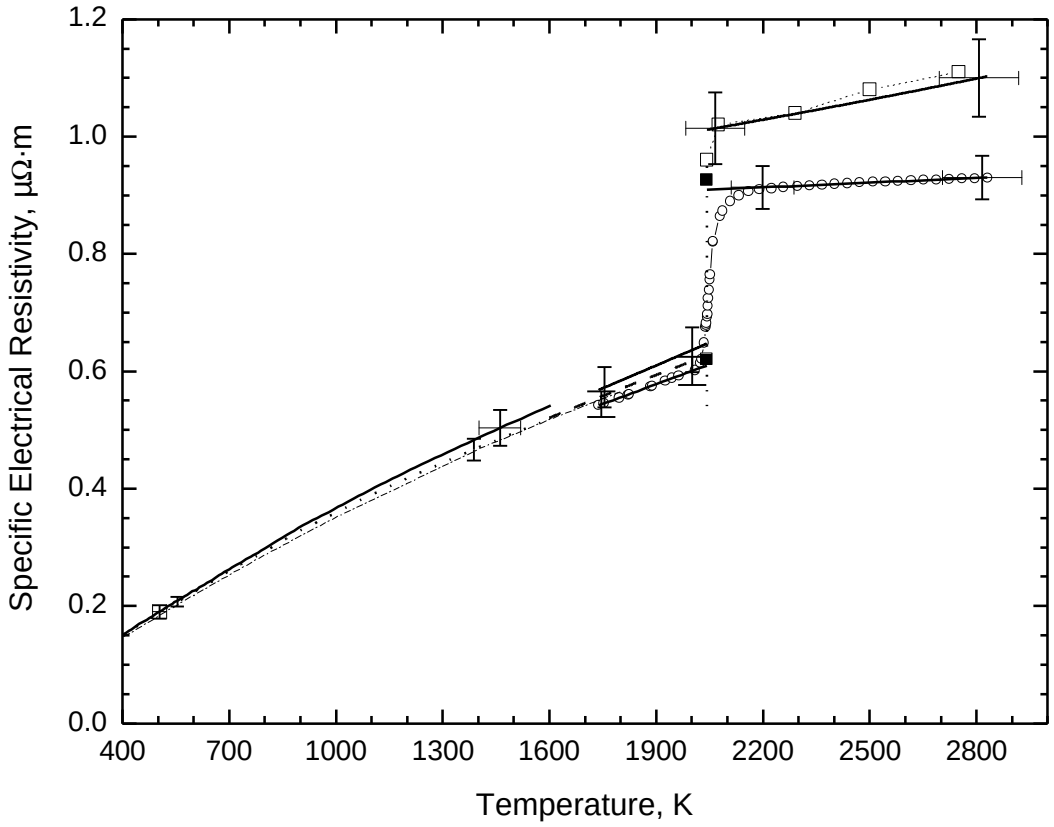

Fig. 2: Electrical resistivity of platinum resistivity without taking actual volume in account, and with volume expansion taken into consideration, versus temperature for platinum. Open circles represent measured data from this work (average of 11 measurements). Full line: linear least-squares fits; dashed-dotted line: literature values from Zinov'yev [25]; full squares: values from Martynyuk [15]; dotted line: measured from this work with temperature from DSC without taking actual volume in account. Solid line: electrical resistively adapted for volume expansion. Both lines are least-squares fits to measured data. Vertical dashed line: end of values measured and calculated with DSC-data (1573 K); vertical dotted line: melting temperature (2042 K); dashed line: literature values from Righini and Rosso [10] without volume correction.

Fig. 2: At the onset of melting (2042 K), which is indicated by a vertical dotted line, we obtain a value of 0.610 µΩ·m and at the end of melting a value of 0.909 µΩ·m, thus an increase of Dr = 0.299 µΩ·m at melting is observed. At 2000 K Righini and Rosso [10] report a value of 0.617 µΩ·m, Martynyuk and Tsapkov [15] report for the onset of melting 0.621 µΩ·m and for the end of melting 0.926 µΩ·m. For the volume considered resistivity values at the onset of melting we obtain a value of 0.647 µΩ·m and at the end of melting a value of 1.012 µΩ·m. An increase of Dr = 0.365 µΩ·m at melting is observed. platinum was the only material where we compared both, resistivity with initial geometry and resistivity with volume expansion considered, to literature values. All measured values give an excellent agreement to the literature values. Based on this results we suggest, that platinum could be used as a calibration substance for pulse-heating-circuits regarding measurements of enthalpy and resistivity.

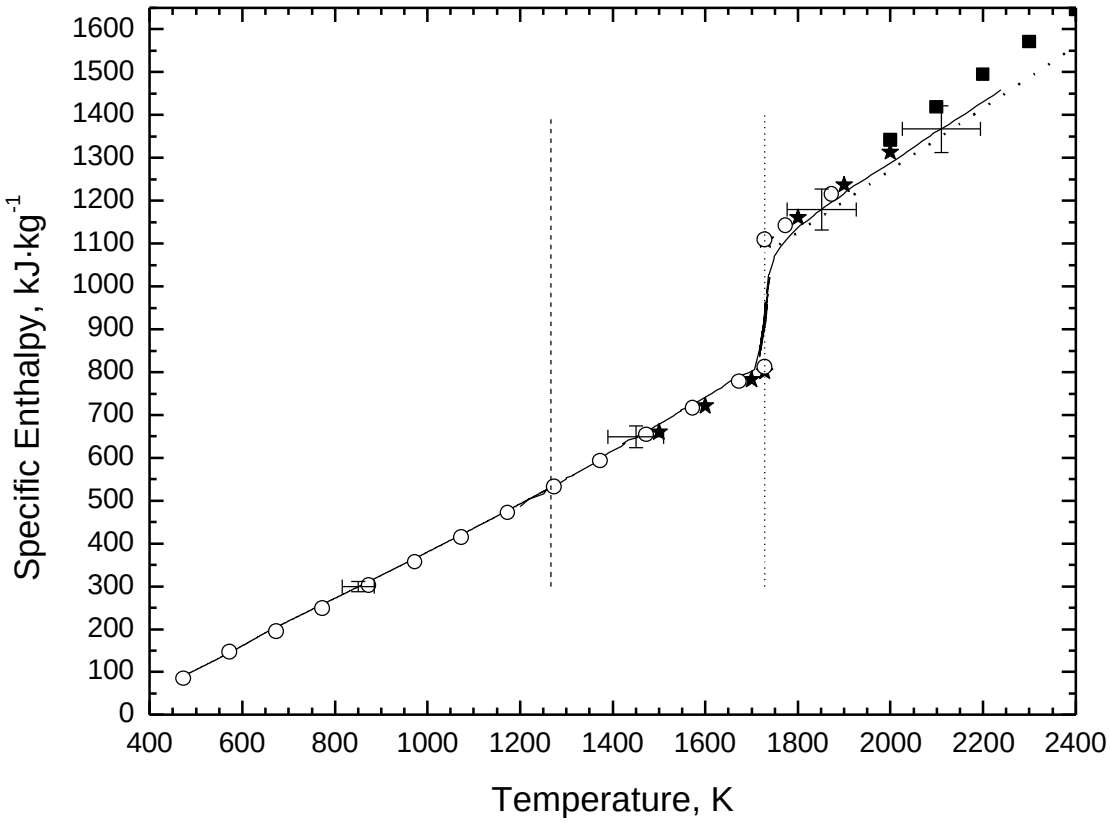

Fig. 3: Specific enthalpy versus temperature for nickel. Full lines represent measured data from this work; vertical dashed line: end of values measured and calculated with DSC-data (1266 K); vertical dotted line: melting temperature (1729 K); open circles: literature values from [26]; full stars: values from [19]; full squares: literature values for the liquid phase from [27]; dotted line: data from [18].

Fig. 3: For solid nickel by pulse-heating in the temperature range 1200 K < T < 1715 K we obtain a c_p of 634.4 J·kg^{-1}·K^{-1} and for the liquid in the temperature range 1740 K < T < 2240 K a c_p value of 797.9 J·kg^{-1}·K^{-1}. Cezairliyan [16] reports: c_p(1700) = 654.8 J·kg^{-1}·K^{-1} and Hultgren [11] gives c_p(*1726*) = 734.8 J·kg^{-1}·K^{-1}.
The measured values give an good agreement to those of literature.

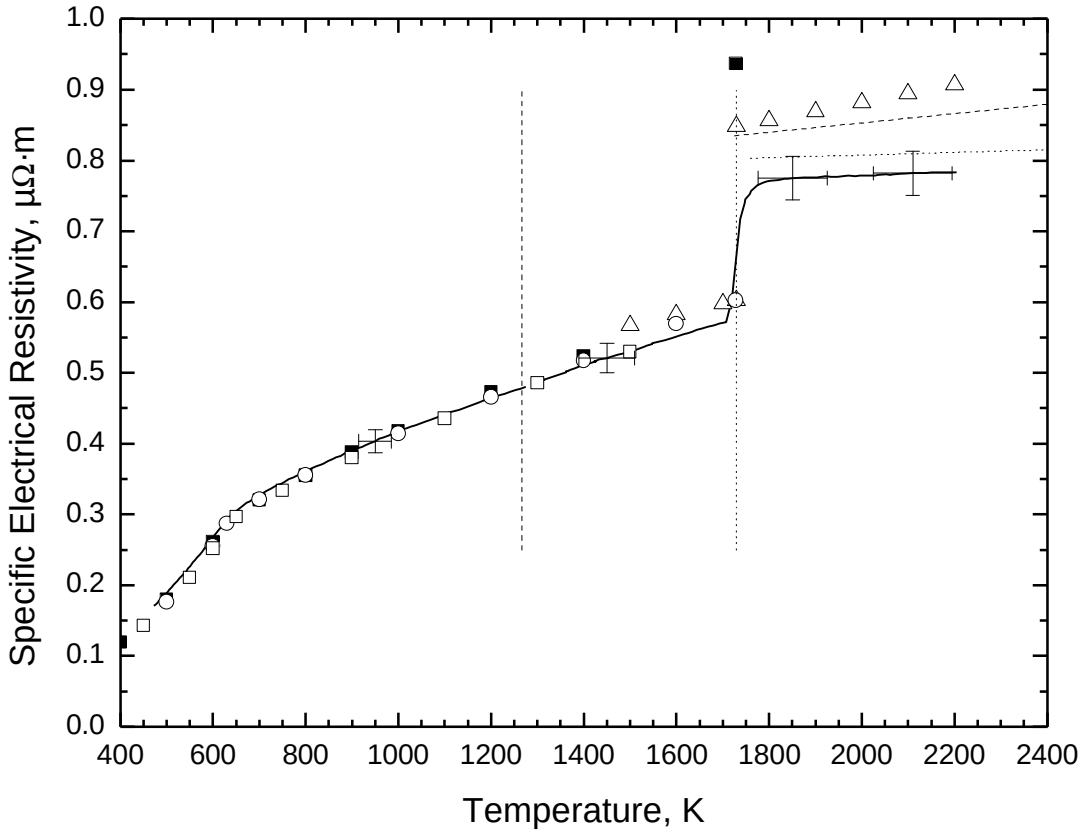

Fig. 4: Electrical resistivity of nickel without taking actual volume in account versus temperature. Full line represent measured data from this work; vertical dashed line: end of values measured and calculated with DSC-data (1266 K); vertical dotted line: melting temperature (1729 K); full sqares: values from Zinov'yev [25] in the solid phase; open squares: data from Maglic [28]; open circle: values from Touloukian [29]; open triangle: values from [19]; dashed line: values for the liquid phase from [30]; dottet line: data from [18]; full star: value at melting temperature in the liquid phase from Hixson [17].

Fig. 4: At the onset of melting, which is indicated with a vertical dotted line, we obtain a value of 0.576 µΩ·m and at the end of melting a value of 0.772 µΩ·m, thus an increase of Dr = 0.196 µΩ·m at melting is observed. At 1700 K [16] report a value of 0.596 µΩ·m for the solid phase, [17] reports 0.937 µΩ·m at 1729 K and [18] has measured 0.790 µΩ·m at 1729 K.

The measured values give good agreement to literature values in the solid phase, whereas in the liquid phase quite a spreading of data can be observed. It should be noticed that recent measurements tend to lower resistivity values in the liquid phase, even when compared to earlier measurements of the same laboratory [18], [19]. Up to now we could not find a reasonable explanation for this behaviour, as other materials e.g. molybdenum [20] that also have been recently re-measured, did not show discrepancies in the liquid resistivity data.

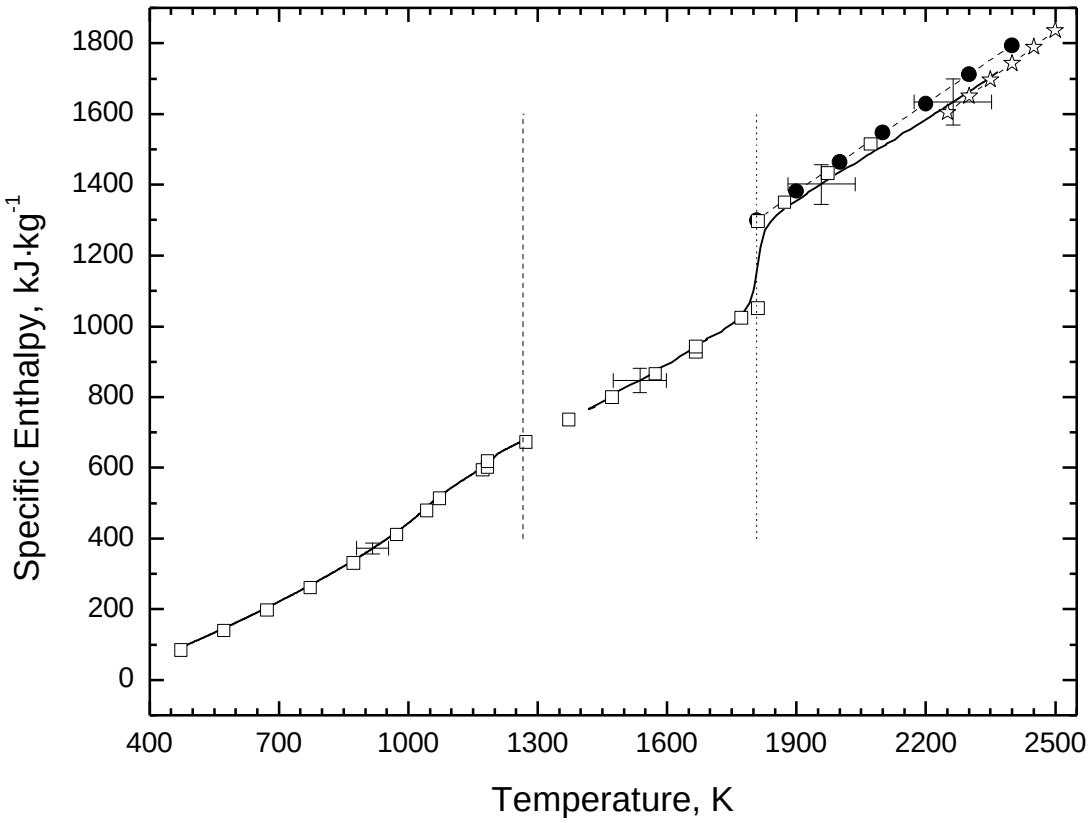

Fig. 5: Specific enthalpy versus temperature for iron. Full lines represent measured data from this work; vertical dashed line: end of values measured and calculated with DSC-data (1266 K); vertical dotted line: melting temperature (1808 K); open square: literature values from C. Mills [26]; full circle: date from the liquid phase from [22]; open star: high temperature values from [27].

Fig. 5: In the temperature range 1420 K < T < 1790 K we obtain for solid iron a c_p of 728.8 J·kg^{-1}·K^{-1} and for the liquid in the temperature range 1830 K < T < 2370 K a c_p value of 766.4 J·kg^{-1}·K^{-1}, literature values are: c_p(*1800)* = 799 J·kg^{-1}·K^{-1} from Cezairliyan [7] and c_p(*1809*) = 824.7 J·kg^{-1}·K^{-1} from Hultgren [21].
The measured values give an good agreement to literature values.

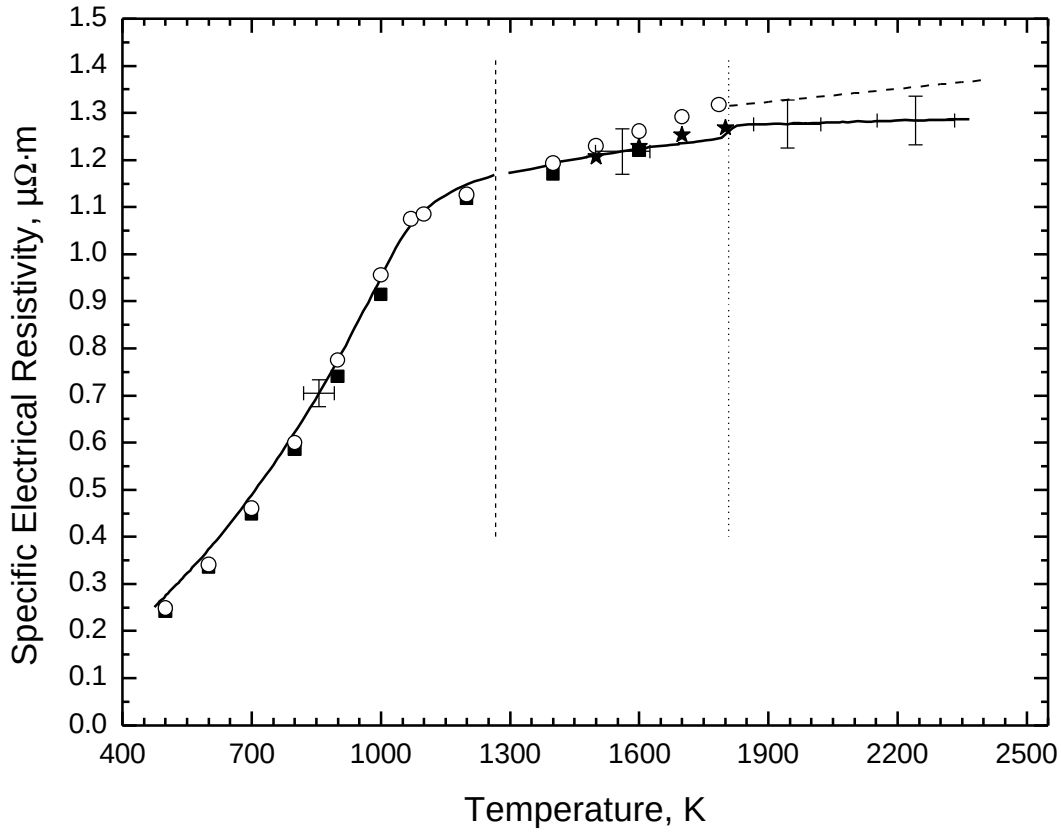

Fig. 6: Electrical resistivity of iron without taking actual volume in account versus temperature. Full line represent measured data from this work; vertical dashed line: end of values measured and calculated with DSC-data (1266 K); vertical dotted line: melting temperature (1808 K); open circle: literature data from Touloukian [31]; full square: values for the solid phase from Zinov'yev [25]; full star: data from [32]; dashed line: data for liquid iron from [30].

Fig. 6: At the onset of melting, which is indicated with a vertical dotted line, we obtain a value of 1.244 µΩ·m and at the end of melting a value of 1.275 µΩ·m, thus an increase of Dr = 0.031 µΩ·m at melting is observed. At 1800 K [7] report a value of 1.269 µΩ·m for the solid phase and [22] report $r_{IG}(1808)$ = 1.29 µΩ·m for the liquid. Our values give a good agreement to literature values, but as mentioned above, recent measurements in the liquid phase tend to lower resistivity values.

5 UNCERTAINTY

According to the guide to the expression of uncertainty in measurement [23] uncertainties reported here are expanded relative uncertainties with a coverage factor of k = 2. An evaluated set of uncertainties is given, for the measured data the following uncertainties are estimated: current, I, 2%; voltage drop, U, 2%; temperature, T, 4%, normal spectral emissivity, e, 6%; mass m, 2%, from which we obtain for enthalpy, H, 4%; enthalpy of melting DH, 8%, specific heat capacity c_p, 8%, specific electrical resistivity with initial geometry, $r_{el,\ IG}$, 4%, specific electrical resistivity with volume expansion considered, $r_{el,\ VOL}$, 6%.

6 CONCLUSION

Within this work temperature dependencies of enthalpy and electrical resistivity of the metals Fe, Ni and Pt have been reported and compared to literature-values. The temperature dependencies could be down scaled to a temperature of about 500 K. Despite the different heating rates both methods used give a very good agreement of the obtained thermophysical data within the stated uncertainties of each experiment and proof that the values obtained by fast pulse-heating under certain circumstances still can be considered to be quasi-static. The fast pulse heating technique can suppress phase transformations in the solid phase [24] and by means of pulse heating obtained values could be a straight continuation of the former phase. Therefore one has to be very careful in data evaluation, and all data have to be compared with quasistatic methods. Melting establishes equilibrium and in the liquid phase the values will be again close to thermodynamic equilibrium.

Acknowledgment
This work was supported by the “Fonds zur Förderung der wissenschaftlichen Forschung”, grant No.: P15055.

REFERENCES

1 Kaschnitz, E. Pottlacher, G., and Jäger, H., *Int. J. Thermophys*. **13** 699, (1992).
2 G. Pottlacher, E. Kaschnitz and H. Jäger, *J. Non-Cryst. Solids*, **156-158**, 374 (1993).
3 C. Cagran, C. Brunner, A. Seifter and G. Pottlacher, *High Temp. High. Press.*, 15th ECTP, paper in print, (2002).
4 A. Seifter, S. Krishnan, G. Pottlacher, contribution presented at TEMPMEKO 2001 in Berlin.
5 A. Cezairliyan, J. L. McClure and C. W. Beckett, *J. Res. Nat. Bur. Stand. (US)*, **75A**, 1 (1971).
6 A. Cezairliyan and A. P. Miiller, *Int. J. Thermophys.*, **5(3)**, 315, (1984).
7 A. Cezairliyan and J. L. McClure, *J. Res. Nat. Bur. Stand. (US)*, **78A**, 1 (1974).
8 Baykara T., Hauge R. H., Norem N., Lee P., Margrave J. L., *High Temperature Science*, **32**,113 (1991).x02 A. Cezairliyan, McClure, *J. Res. Nat. Bur. Stand. (US)*, **78A**: (1),1 (1974).
9 Seville A. H., *J. Chem. Thermodynamics*, **7**, 383 (1975).
10 Righini F., Rosso A., High Temp. - High Press., **12**, 335 (1980).
11 Hultgren R., Desai P. D., Hawkins D. T., Gleiser M., Kelley K. K., Wagman D. D., *Selected Values of the Thermodynamic Properties of the Elements*, American Society for Metals (1973).
12 Margrave J. L., *High Temp. - High Press.*, **2**, 583 (1970).
13 Chaudhuri A. K., Bonell D. W. Ford L. A., and Margrave J. L., *High Temperature Science*, **2**, 203 (1970).
14 Hixson R. S., Winkler M. A., Int. J. Thermophys, **14**, 409 (1993).
15 Martynyuk M. M., Tsapkov V. I., Fiz. Metal. Metalloved., **37**, 49 (1974).
16 A. Cezairliyan and A. P. Miiller, *Int. J. Thermophys.*, **4**, 289 (1983).

17 R. S. Hixson, M. A. Winkler and M. L. Hodgdon, *Phys. Rev. B*, **42**, 6485 (1990).
18 A. Seifter, PhD. Thesis, TU-Graz, 156 (2001).
19 W. Obendrauf, *Strahlungsmessung an stoßaufgeheizten Drahtproben, diploma thesis*, Technical University Graz, Austria (1991).
20 C. Cagran, B. Wilthan and G. Pottlacher, Normal Spectral Emissivity at a Wavelength of 684.5 nm and Thermophysical Properties of Solid and Liquid Molybdenum, presented at FIFTEENTH SYMPOSIUM ON THERMOPHYSICAL PROPERTIES, BOULDER (2003).
21 R. Hultgren, P. D. Desai, D. T. Hawkins, M. Gleiser, K. K. Kelley and D. D. Wagman, *Selected Values of the Thermodynamic Properties of the Elements*, American Society for Metals, UMI, Reprinted (1990).
22 M. Beutl, G. Pottlacher and H. Jäger, *Int. J. Thermophys.*, **15**, 6, 1323 (1994).
23 Expression of the Uncertainty of Measurement in Calibration, EA-4/02, http://www.european-accreditation.org/pdf/EA-4-02ny.pdf.
24 Seifter, A., Pottlacher, G., Jäger H., Groboth G., and Kaschnitz E., Ber. Bunsenges. *Phys. Chem*. **102**, 1266 (1998)
25 Zinov'yev V. E., *Metals at High Temperatures - Standard Handbook of Properties*, National Standard Reference Data Service of the USSR, Hemisphere Publishing Corporation (1990).
26 K. C. Mills, B. J. Monaghan and B. J. Keene, *Thermal Conductivities of Molten Metals – Part 1: Pure Metals*, NPL Report CMMT(A) 53 (1997).
27 G. Pottlacher, H. Jäger, T. Neger, *High Temp.-High Press.* **19**,19 (1987).
28 K. D. Maglic, A. S. Dobrosavljevic, N. Lj. Perovic, *The Experimental Study of Transport and Thermodynamic Properties of Nickel*, Plenum Press, 81 (1988).
29 Y. S. Touloukian, *Properties of selected Ferrous Alloying*, McGrawn-Hill/CINDAS Data Series on Material Properties Vol. III-1 (1971).
30 U. Seydel and W. Fucke, *Z. Naturforsch.*, **32a**, 994 (1977).
31 Y. S. Touloukian, R. W. Powell, C.Y. Ho and P. G. Klemens, ed., *Thermophysical Properties of High Temperature Solid Materials* – Vol. 1-PT 1, (1967).
32 A. Cezairliyan and J. L. McClure, Thermophysical Measurements on Iron Above 1500 K Using a Transient (Subsecond) Technique, Inst. f. Material Research, NBS (1973).